Spatial Dynamics of VCSEL Arrays

Peter M. Goorjian*[a], C. Z. Ning[b], Govind P. Agrawal[c]
[a]NASA Ames Research Center, M.S. 202A-1, Moffett Field, CA 94035-1000
[b]NASA Ames Research Center, M.S. T27A-1, Moffett Field, CA 94035-1000
[c]The Institute of Optics, University of Rochester, Rochester, NY 14627

ABSTRACT

Numerical simulations of the spatial dynamics of the light output of two-dimensional arrays of VCSELs are presented. The cases presented include square and circular arrays of nine elements. For both configurations the spacing between elements is varied to study the effects on the interaction between elements. In addition, the effects of index guiding on the supermodes of the arrays will be shown. It was found that, with only a small amount of index guiding, the interactions between elements of the VCSEL array are effectively eliminated for all spacings between elements. The time evolutions of the spatial profiles of the laser intensity and carrier density are obtained by solving the Effective Semiconductor Bloch-Maxwell equations by a finite-difference algorithm. The algorithm can handle devices with multiple active regions of any shapes or pattern. There is no a priori assumption about the type or number of modes.

Keywords: VCSELs, laser arrays, spatial dynamics, computational modeling, optoelectronics, laser optics

1. INTRODUCTION

Two-dimensional arrays of vertical-cavity surface-emitting lasers (VCSELs) are important for producing high-intensity light[1–3] and for tailoring the far-field intensity distribution for applications. Complex spatial dynamics have been observed experimentally when the injected current is high[3] with the laser output jumping between different mode patterns. This jumping was attributed to spatial hole burning. In this paper, numerical simulations of the spatial dynamics of the interactions between array elements are presented. The model can account for the effects of spatial hole burning.[4] The cases to be presented include square and circular arrays of VCSELs. For both configurations the spacing between elements is varied to study the effects on the interaction between elements. In addition, the effects of index guiding on the supermodes of the arrays will be shown.

The spatial dynamics of the VCSEL arrays are modeled by an approximation to the semiconductor Maxwell–Bloch equations.[5] The time evolution of the spatial profiles of the laser and carrier density is obtained by solving these partial differential equations by a finite-difference algorithm. The algorithm is fairly general; it can handle devices with one or multiple active regions of any shapes, which can be either gain or index guided. There is no a priori assumption about the type or number of modes.The physical modeling includes the effects of nonlinear carrier dependence and dispersion with respect to wavelength on the optical gain and refractive index. The modeling[5–7] of the optical susceptibility is based on first-principles and includes device details such as a quantum well structure and many-body effects. Temporal dynamics as fast as on a picosecond scale can be resolved. In this paper, the VCSELs are based on InGaAs/GaAs quantum well structures.

* email: goorjian@nas.nasa.gov, cning@nas.nasa.gov, gpa@optics.rochester.edu

Physics and Simulation of Optoelectronic Devices IX, Yasuhiko Arakawa, Peter Blood, Marek Osinski,
Editors, Proceedings of SPIE Vol. 4283 (2001) © 2001 SPIE · 0277-786X/01/$15.00

2. GOVERNING EQUATIONS

The effective Maxwell–Bloch Equations can be written as:[5,6]

$$\frac{n_g}{c}\frac{\partial E}{\partial t} = \frac{i}{2K}\nabla_\perp^2 E - \kappa E + \frac{iK\Gamma}{2\epsilon_0\epsilon_b}P + \frac{i\delta n(x,y)}{n_b}KE \tag{1}$$

$$\frac{\partial N}{\partial t} = D_N \nabla_\perp^2 N - \gamma_n N + \frac{\eta J(x,y,t)}{e} + \frac{L\Gamma}{2}\frac{i}{4\hbar}(P^*E - PE^*) \tag{2}$$

$$P = P_0 + P_1 \tag{3}$$

$$P_0 = \epsilon_0\epsilon_b\chi_0(N)E \tag{4}$$

$$\frac{dP_1}{dt} = -\Gamma_1(N)P_1 + i(\omega_c - \omega_1(N))P_1 - i\epsilon_0\epsilon_b A_1(N)E \tag{5}$$

Here E is the complex laser field envelope amplitude, N is the total carrier density, P_0 and P_1 are the effective material polarization functions that have been constructed from microscopic theory,[5] and $J(x,y,t)$ is the pumping current density. Further, $\delta n(x,y)$ is the guiding index profile arising from, e.g., oxide confinement, $\nabla_\perp^2$ is the Laplacian in the transverse plane, c is the speed of light, ϵ_0 is the permittivity of free space, ω_c is the optical carrier wave frequency in radians per seconds, n_b is the background index of refraction, n_g is the group index of refraction, $\epsilon_b = n_b^2$ is the background relative permittivity, $\mathrm{K} = \omega_c n_b/c$ is the optical wavenumber in the cavity with a background index of refraction n_b, κ is the cavity loss, D_N is the carrier diffusion coefficient, γ_n is the nonradiative decay constant or carrier loss rate due to spontaneous and nonradiative processes, η is the quantum efficiency, e is the electron charge, $\hbar = h/2\pi$, where h is Planck's constant, Γ is the confinement factor, and L is the cavity length.

Many-body effects are contained in the density-dependent coefficients $\chi_0(N)$, the effective background susceptibility, $\Gamma_1(N)$, the gain bandwidth, $\omega_1(N)$, the detuning, and $A_1(N)$, the strength of the Lorentzian oscillator. The derivation of these four density-dependent coefficients, which model the optical susceptibility $\chi(\omega, N)$, is given in References 5 and 6.

The simulations were conducted for arrays of VCSELs operating at 980 nm with circular current apertures of 5.6 μm in diameter. The cavity length L was 144 nm, the carrier diffusion coefficient was 20 cm^2/s and the confinement factor Γ was 0.25. The three parameters most important in determining the dynamics are the three decay rates Γ_1, κ, and γ_n. The inverse values of these parameters set the relevant time scales. In our calculations, $1/\Gamma_1(N)$ was approximately 15 fs, (the material polarization P_1 changed on that time scale). Introducing the scaled cavity loss as $\tilde{\kappa} = \kappa/(n_g/c)$, the photon lifetime, $1/\tilde{\kappa}$, was about 2 ps. Finally, the carrier lifetime, $1/\gamma_n$ was 2 ns. At the nanosecond time scale, the time averages laser field was essentially steady for these calculations.

3. COMPUTED RESULTS

Computed results are presented for square and circular VCSEL arrays of nine elements each. For the square array, the current density at each VCSEL was set at 1.73 kiloamps per cm sq, and the separation between element centers was 6.6, 7.6, 8.6 and 9.6 μm. For the circular array, the current density at each VCSEL was set at 1.15 kiloamps per cm sq. Results are shown in which the diameter of the circle on which the element centers are located was 22.4 and 19.2 μm. For all cases, both gain guiding and index guiding were used, (for index guiding a change of refractive index of 0.005 was used). The initial light and carrier density fields were determined under conditions in which there were no interactions between elements. In the figures, the spatial profiles of the intensities of the laser (top row) and carrier density (bottom row) fields are shown with time averaged (periods indicated) light fields and instantaneous (at the end of the light field period above) carrier density fields.

3.1. Square Array; Gain Guided

Figure 1 shows two consecutive light fields averaged over two hundred picoseconds and a light field averaged over four nanoseconds, as indicated in the figure. While there is light dynamics on the shorter time scale due to interactions between the array elements, on the longer time scale, the resulting intensity pattern is static with an enhanced light output from the center element. As might be expected, the carrier density field below the center element is the most depleted.

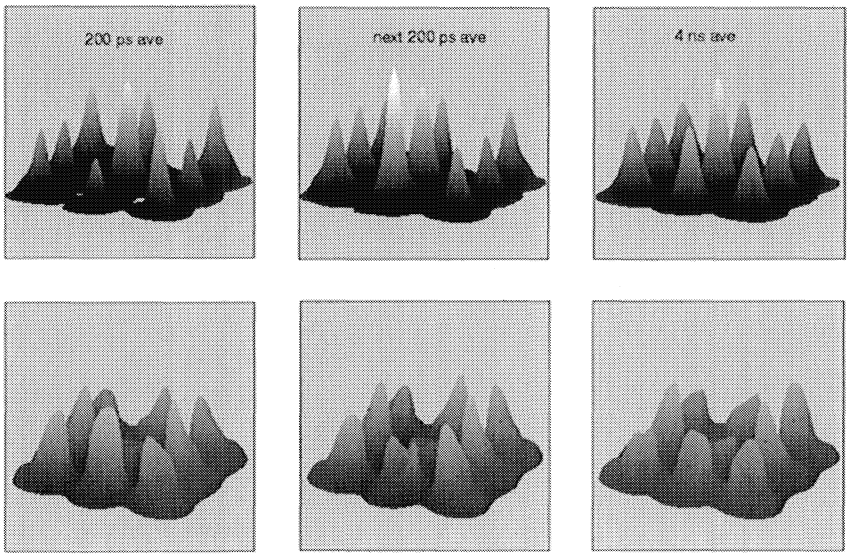

Fig. 1. The light intensity (top row) and carrier density (bottom row) fields of a square array of nine VCSELs, element centers separated by 9.6 μm, no index guiding.

3.2. Ring Array; Gain Guided

Figure 2 shows two consecutive light fields averaged over two hundred picoseconds and a light field averaged over four nanoseconds. Initially the light field is symmetric, but it evolves into an asymmetric pattern that is maintained over the longer time scale. The asymmetry is reflected in the carrier density field.

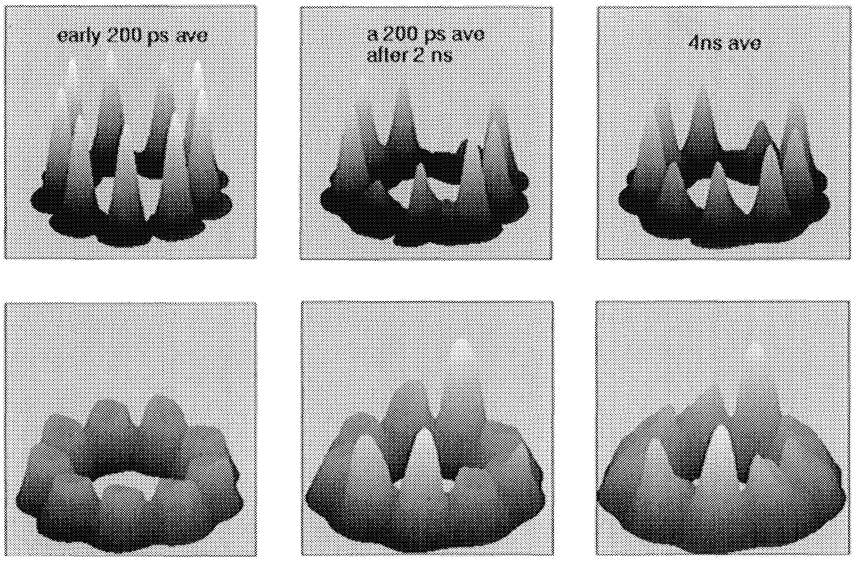

Fig. 2. The light intensity (top row) and carrier density (bottom row) fields of a ring array of nine VCSELs, ring diameter is 22.4 μm, no index guiding.

3.3. Square Array; Gain Guided; Various Element Separations

Figure 3 shows the effects of decreasing the separation between elements, with the interactions becoming stronger until they are acting essentially as one large VCSEL.

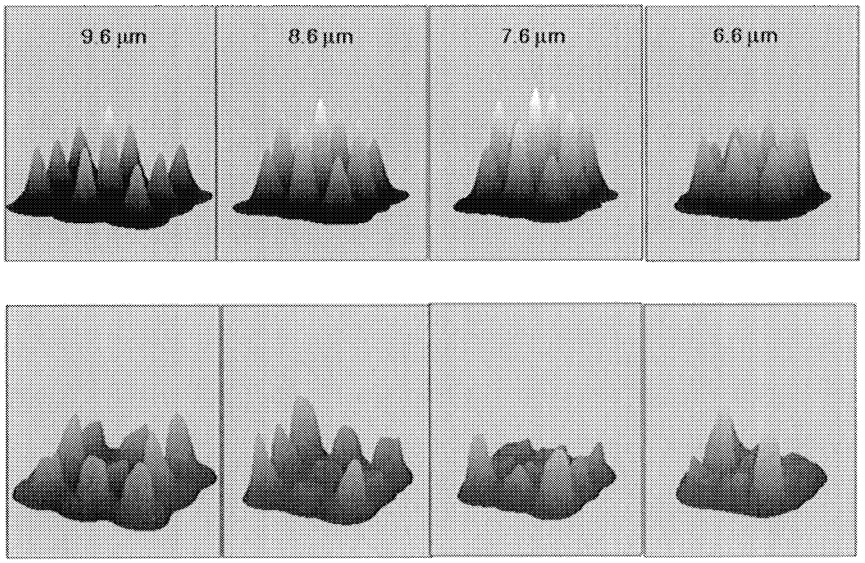

Fig. 3. Comparison of four separation distances, 9.6 μm, 8.6 μm, 7.6 μm, and 6.6 μm; all light fields are four nanosecond averages.

3.4. Ring Array; Gain Guided; Two Ring Diameters

Figure 4 shows the effects of decreasing the ring diameter, with the light field again an asymmetric pattern. The carrier density field shows a strong peak where the light field has been suppressed due to the interaction of the VCSELs.

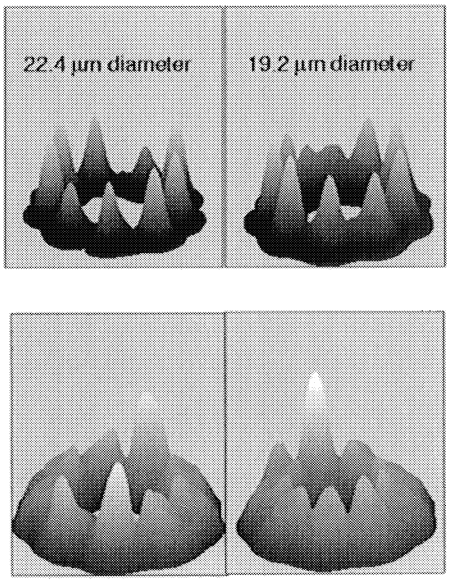

Fig. 4. Comparison of two ring diameters, 22.4 μm, and 19.2μm; all light fields are four nanosecond averages.

3.5. Square Array; Effects of Index Guiding

Figures 5 and 6 shows the effects of index guiding on the interaction between the elements for various distances of element separation. Now the elements act essentially independently, although there is some slight interaction as can be seen in the carrier density fields. Also the peaks in the carrier density fields have craters, which are a result of spatial hole burning in producing the peaks in the light fields.

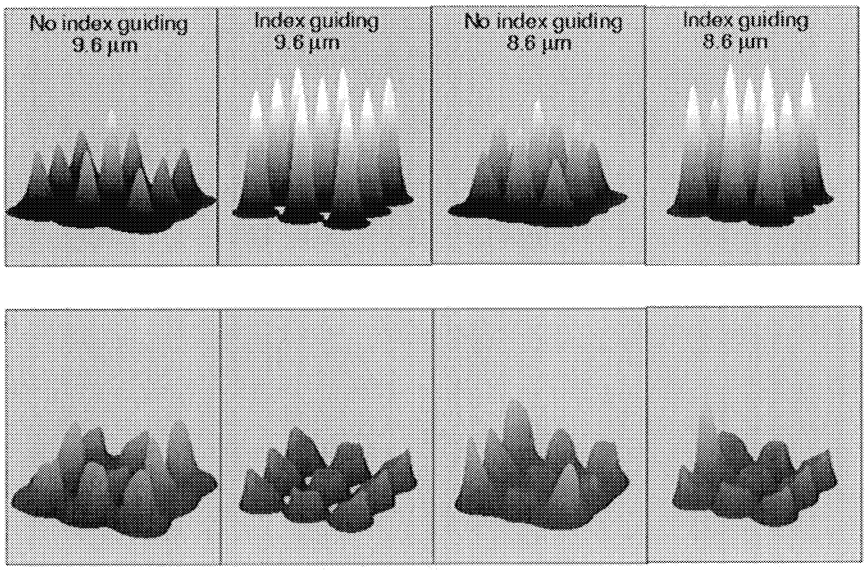

Fig. 5. Comparison of no index guiding and index guiding at separation distances, 9.6 μm, and 8.6 μm.

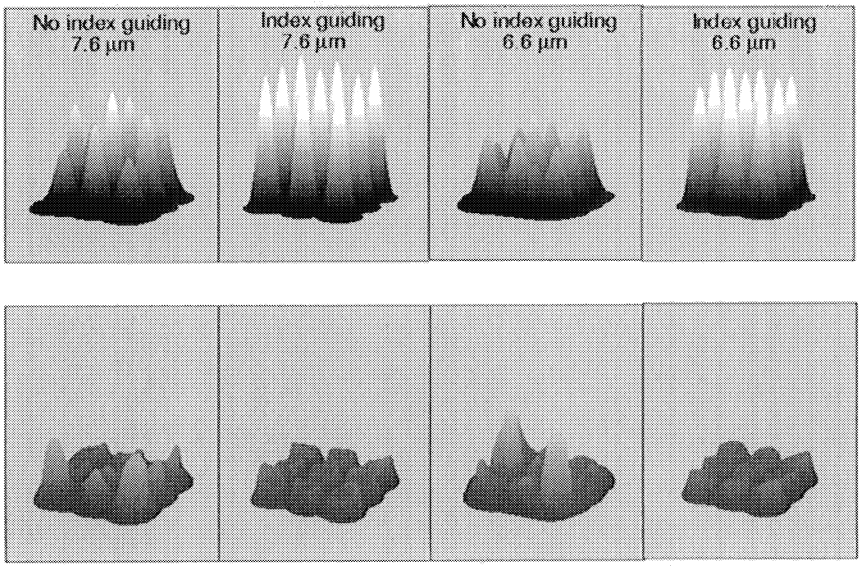

Fig. 6. Comparison of no index guiding and index guiding at separation distances, 7.6 μm, and 6.6 μm.

3.6. Ring Array; Effects of Index Guiding

Finally, Figure 7 shows the effects of index guiding on the interaction between the elements for the two diameters. As in the square array case, the elements act essentially independently. Again there are craters in the carrier density fields, which are a result of spatial hole burning.

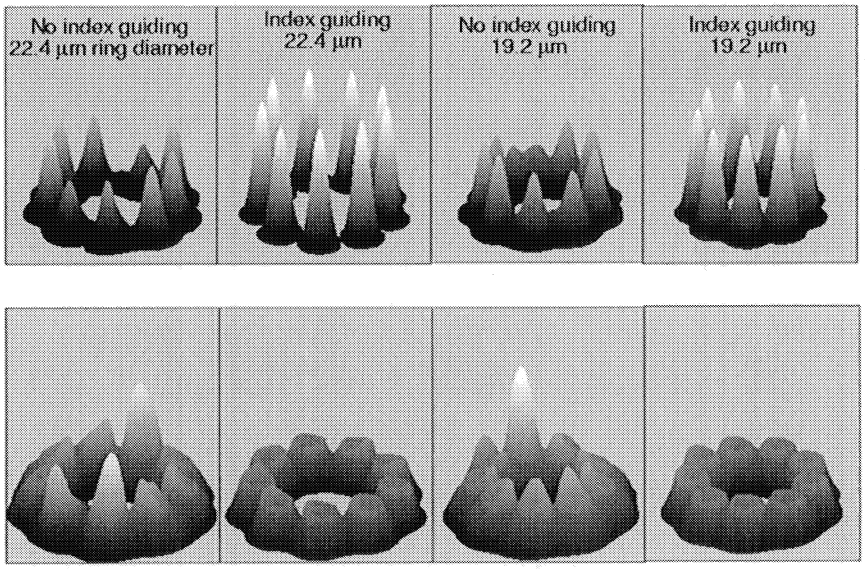

Fig. 7. Comparison of no index guiding and index guiding at ring diameters 22.4 μm, and 19.2μm.

4. CONCLUSION

A new algorithm has been developed for modeling the spatial dynamics of the light field of two-dimensional arrays of vertical-cavity surface-emitting lasers. The model can account for the effects of spatial hole burning. Two types of arrays were studied: (1) a square array of nine elements and (2) an array of nine elements in a circle. In both cases the spacing between elements was varied to see the effects on the pattern of the light output in the near field. The results showed that as the elements were brought closer together the light fields became coupled so that the light intensities at some elements were enhanced while at other elements they were diminished. However, by adding only a small amount of index guiding (refractive index change of 0.005), the interactions between elements of the VCSEL array were effectively eliminated for all spacings between elements.

REFERENCES

1. M. Orenstein, and T. Fishman, "Supermodes of Hermite Tapered Arrays of Vertical-Cavity Semiconductor Lasers," *IEEE J. Quanum Electron.*, **35**, 1062-1066 (1999).
2. D. Natan, M. Margalit, and M. Orenstein, "Localization immunity and coherence of extended two-dimensional semiconductor vertical cavity-locked laser arrays," *J. Opt. Soc. Am. B*, **14**, 1501-1504, (1997).
3. T. Fishman, and M. Orenstein, "Cyclic vertical cavity semiconductor laser arrays with odd numbers of elements: lasing modes and symmetry breaking," *Opt. Lett.* , **21**, 600-602, (1996).
4. P. M. Goorjian, C. Z. Ning, and G. P. Agrawal, "Transverse mode dynamics of VCSELs undergoing current modulation," Paper 3944-30,, Physics and Simulation of Optoelectronic Devices VIII, Photonics West, 2000, (SPIE), San Jose, CA, January 22-28, 2000.
5. C. Z. Ning, R. A. Indik and J. V. Moloney, "Effective Bloch-equations for semiconductor lasers and amplifiers," *IEEE J. Quanum Electron.*, **33**, 1543-1550, (1997).
6. P. M. Goorjian and C. Z. Ning, "Transverse mode dynamics of VCSELs through space-time simulation," *Optics Express*, **5**, 55-62, (1999). Also animations of solutions available on http://www.nas.nasa.gov/~goorjian/Pub/pub.html
7. C. Z. Ning and P. M. Goorjian, "Microscope modeling and simulation of transverse mode dynamics of vertical-cavity surface-emitting lasers," *J. Opt. Soc. Am. B*, **16**, 2072-2082, (1999).